Neuroscience 593 (2026) 87–95

Contents lists available at ScienceDirect

Neuroscience

journal homepage: www.elsevier.com/locate/nsc

Doublecortin-expressing cells are selectively altered in the piriform cortex but not in neurogenic areas of symptomatic *Mecp2*-heterozygous mice

Rafael Esteve-Pérez [a,1], Paloma Sevilla-Ferrer [a,1], Enrique Lanuza [a], Vicente Herranz-Pérez [a,b], Jose V. Torres-Pérez [a], Carmen Agustín-Pavón [a,*]

[a] Departament de Biologia Cel·lular i Biologia Funcional, Universitat de València, Spain
[b] Centro de Investigación Biomédica en Red de Enfermedades Neurodegenerativas (CIBERNED)-ISCIII, Madrid, Spain

ARTICLE INFO

Keywords:
Neurodevelopmental disorders
Neurogenesis
Olfactory system
Rett syndrome

ABSTRACT

Rett Syndrome (RTT) is a neurodevelopmental disorder which mainly affects girls, leading to profound impairments in motor function, loss of speech, intellectual disability, and epilepsy, among other symptoms. Most cases are caused by mutations in the X-linked *MECP2* gene, which encodes the methyl-CpG-binding protein 2 (MeCP2), an epigenetic reader with a crucial function in the regulation of neural maturation. Previously, using the marker of immature neurons doublecortin (DCX), we showed that a population of embryonic-born neurons of the piriform cortex, which experience prolonged maturation throughout life, was increased in the piriform cortex of symptomatic young adult (2 months old) *Mecp2*-null male mice. By contrast, these cells were not affected in age matched *Mecp2*-heterozygous female mice, who are pre-symptomatic at that age. To determine whether symptom onset would affect DCX-expressing neurons, in this study we analysed samples from 6 months old, symptomatic *Mecp2*-heterozygous female mice. Our results show a specific increase in the density of DCX-positive neurons in the piriform cortex, consistent with observations in males. However, no differences were detected in the neurogenic niches of the dentate gyrus or the ventricular-subventricular zone when compared to their wild-type controls. Further, morphological analyses of the DCX-expressing cells of the piriform cortex reveal that they are smaller and show less complex dendritic branching in mutant mice. In conclusion, our findings support a role of MeCP2 in the maturation process of the embryonic-born DCX neurons in the piriform cortex and point to region-specific alterations in neuronal maturation in RTT.

Introduction

Rett syndrome (RTT) is a rare neurodevelopmental disorder that affects mainly females, characterised by a developmental regression occurring between 6 to 18 months of age, leading to loss of speech, intellectual disability, repetitive hand movements, breathing abnormalities, and motor impairment, among other symptoms (Amir et al. 1999). The main cause of classical RTT are loss-of-function mutations in the X-linked *MECP2* gene, encoding the methyl-CpG-binding protein 2 (MeCP2) (Amir et al. 1999). In males, hemizygous loss-of-function *MECP2* mutations are typically lethal, resulting in severe neonatal encephalopathy and often perinatal death (Santos et al. 2009), whereas mutations and variants not leading to complete loss of function in this gene have been linked to disorders causing intellectual disability, neuroendocrine dysfunction or psychiatric conditions (Moretti and Zoghbi 2006; Canton et al. 2023).

Originally identified as a transcriptional repressor (Nan et al. 1997), MeCP2 is currently recognized as a multidomain epigenetic regulator that modulates gene expression in a context-dependent manner, both silencing and promoting transcription (Sharifi and Yasui 2021). Murine models with MeCP2 loss-of-function mutation serve as a valuable approach to understanding the implication of MeCP2 in the nervous system (Guy et al. 2001). In contrast to humans, male mice survive infancy but have a short lifespan and an early onset of symptoms, with animals of 2 months of age being fully symptomatic, whereas females display a variable onset of motor symptoms, being symptomatic by 2 to 6 months of age (Guy et al. 2001; Abellán-Álvaro et al. 2021; Cuitavi et al. 2025). The timing of phenotypic manifestations of RTT in humans and murine models suggests that the underlying cause of symptoms is not an altered developmental neurogenesis, but a disruption in the

* Corresponding author at: Departament de Biologia Cel·lular i Biologia Funcional, Universitat de València, Av. Vicent Andrés Estellés, s/n 46100 Burjassot, Spain.
E-mail address: pavon@uv.es (C. Agustín-Pavón).
[1] These authors contributed equally to the study.

https://doi.org/10.1016/j.neuroscience.2025.12.010
Received 25 September 2025; Accepted 4 December 2025
Available online 7 December 2025

maintenance of a mature neuronal functionality (Shahbazian 2002; Kishi and Macklis 2004; Smrt et al. 2007). This is further supported by the observed pattern of MeCP2 protein expression, characterized by low levels during embryonic brain development and reaching the highest levels in more mature structures (Shahbazian 2002; Kishi and Macklis 2004).

In agreement with a key role of MeCP2 for neuronal maturation, we previously showed that immature neurons, identified by using the marker doublecortin (DCX), were increased in specific brain regions of adolescent and young adult *Mecp2*-null mice (Martínez-Rodríguez et al. 2019; Torres-Pérez et al. 2022). In the brain of healthy, wild-type (WT) rodents, DCX-immunoreactive (DCX-ir) cells are present in neurogenic areas such as the dentate gyrus (DG) of the hippocampus and the ventricular-subventricular zone (V-SVZ), from which neuroblasts migrate mainly through the rostral migratory stream (RMS) to the olfactory bulb (OB) (Doetsch et al. 1999; Whitman and Greer 2009), but also to other locations such as the nucleus accumbens NAc (García-González et al. 2021).

In addition, layer II of the piriform cortex (Pir) harbours a population of DCX-ir cells generated during embryonic development that persists into adulthood (Nacher et al. 2001; Rubio et al. 2016). These cells have been shown to mature gradually with age and integrate as glutamatergic neurons (Rotheneichner et al. 2018; Benedetti et al. 2020). Interestingly, while proliferative neurogenesis seems largely absent postnatally in mammals with larger brains, such as non-human and human primates (Paredes et al. 2016; Sorrells et al. 2018), cortical DCX-ir immature neurons of prenatal origin might be widespread in these species (La Rosa et al. 2020), including humans (Coviello et al. 2022; Li et al. 2023), highlighting the importance of characterising this population in disease models.

Our prior findings revealed that DCX-ir cells of the Pir, and adjacent olfactory tubercle, but not the DG or OB, were significantly increased in young *Mecp2*-null male mice as compared with age-matched WT controls (Martínez-Rodríguez et al. 2019). By contrast, we did not find any effect in any of those regions in young adult *Mecp2*-heterozygous (*Mecp2*-het) females (Martínez-Rodríguez et al. 2019). Since young adult females are largely pre-symptomatic (Cuitavi et al. 2025), we hypothesised that alterations in DCX-ir cells might emerge later, when symptoms are already present in *Mecp2*-het females. To test this hypothesis, here we analysed the density and morphological features of DCX-ir cells across several brain areas, in 6 months old *Mecp2*-het female mice and their WT littermates.

Materials and methods

Animals

For these experiments, we used spared samples from 6 months old female mice of the *Mecp2*$^{tm1.1Bird/J}$ strain (WT, n = 5; *Mecp2*-heterozygous, n = 8, Jackson Laboratory), obtained from symptomatic females used in a previous study (Cuitavi et al. 2025). Mice were housed in standard laboratory cages in groups of 2–5 animals, under controlled humidity and temperature (22 °C), with a 12:12-h light/dark cycle, and water and food available *ad libitum*. For genotyping, we obtained ear punches at weaning, and after DNA extraction, we applied the protocol supplied for this strain by the Jackson Laboratory. The protocols were approved by the Animal Experimentation Ethics Committee of the University of Valencia, Protocol 2019/VSC/PEA/0027, and carried out in strict accordance with EU directive 2010/63/EU.

Perfusion and histology

Animals were deeply anaesthetized using pentobarbital (50 mg/Kg) and transcardially perfused with saline solution followed by 4 % paraformaldehyde in 0.1 M phosphate buffer (PB), pH 7.4. Brains were carefully removed from the skull, postfixed overnight in the same fixative and transferred to 30 % sucrose in 0.01 M phosphate buffered saline (PBS, pH 7.6) until they sank. The brains were then frozen and cut in six series of 40-μm-thick coronal sections with a freezing microtome. Free-floating sections were collected in five parallel series and kept at −20 °C in 30 % sucrose in PB (0.1 M, pH 7.4) for future processing.

Doublecortin immunohistochemistry

We obtained permanent immunostained preparations for DCX in one out of the six parallel series, using the indirect avidin–biotin peroxidase complex/3,3′-diaminobenzidine-staining (ABC/DAB) procedure, as described in our previous work (Martínez-Rodríguez et al. 2019). In brief, brain slices were first incubated with 1 % H_2O_2 in 0.05 M tris-buffered saline (TBS, 0.9 % NaCl in TB) for 30 min at room temperature (RT) to block endogenous peroxidase activity. Subsequently, sections were incubated with 2 % normal horse serum (NHS) and 0.3 % Triton-X100 in 0.05 M TBS pH 7.4 for one hour at RT, to block nonspecific binding. Brain slices were then incubated overnight at 4 °C with a goat primary antibody anti-DCX (C-18, sc:8066, Santa Cruz Biotechnology, Inc) diluted 1:500 in 0.05 M TBS pH 7.4, with 2 % NHS and 0.3 % Triton-X100. The next day, sections were incubated for two hours at RT with biotinylated horse anti-Goat-IgG secondary antibody (BA-9500, Vector) diluted 1:200 in the same buffer. Afterwards, sections were incubated for 90 min at RT in ABC (Vector) in TBS with 0.3 % Triton-X100. Sections were thoroughly washed in TBS (3 x 10 min.) between each step. To reveal peroxidase activity, sections were incubated for five minutes in DAB-SigmaFAST (Sigma) in TB. Sections were mounted using 0.2 % gelatine in TB, dehydrated with alcohol, cleared with xylol and cover-slipped with Entellan.

Image acquisition

We analysed the samples with a Leica Leitz DMRB microscope, equipped with a digital camera (Leica DFC495) and Motic Software at *a priori* selected Bregma levels (B), according to (Paxinos and Franklin, 2012). For the piriform cortex (Pir), we analysed three brain sections at the approximate bregma levels B0, B-1 and B-2 mm, taking one representative picture at 20x magnification for each hemisphere; similarly, for the dentate gyrus of the hippocampus (DG), we analysed three sections at the bregma levels B-1, B-2 and B-3 mm, again taking one picture at 20X for each hemisphere. In those regions, DCX-ir cells could be clearly differentiated from background staining and individual cells could be counted (Supplementary Fig. 1, A, B). Immunostaining using the DAB technique followed by conventional microscopy is not suitable to analyse individual cells of granular cell layer of the OB, due to the high density of cells and fibres; thus, we analysed DCX-ir cells from the periglomerular region only, by taking at least three pictures at 10X magnification for each animal from bregma levels B4.8 to 3.56 (Supplementary Fig. 1, C). Similarly, the DAB technique is not suitable to analyse individual DCX-ir cells in the lateral wall of the lateral ventricles (Supplementary Fig. 2), so we analysed the possible migration of V-SVZ generated DCX-ir cells to the striatum. In this region, we only could individualize DCX-ir cells migrating from the ventral tip of the V-SVZ into the nucleus accumbens (NAc), whereas there were no recognisable cells with neuronal morphology migrating toward the caudatus putamen (CPu) from the dorsal region (Supplementary Fig. 2). Thus, we took one picture per hemisphere at 20X magnification in the ventral V-SVZ – NAc region, from approximately B1 to B0.6 mm (Paxinos and Franklin 2019).

Quantification of DCX-immunoreactive cells

In the Pir, an experimenter who was blind to the genotype of the mice inspected the sections and counted the number of cells in each area. DCX-ir cells have been previously classified into two populations based on size and morphology: (1) “simple”, small cells without neurites or

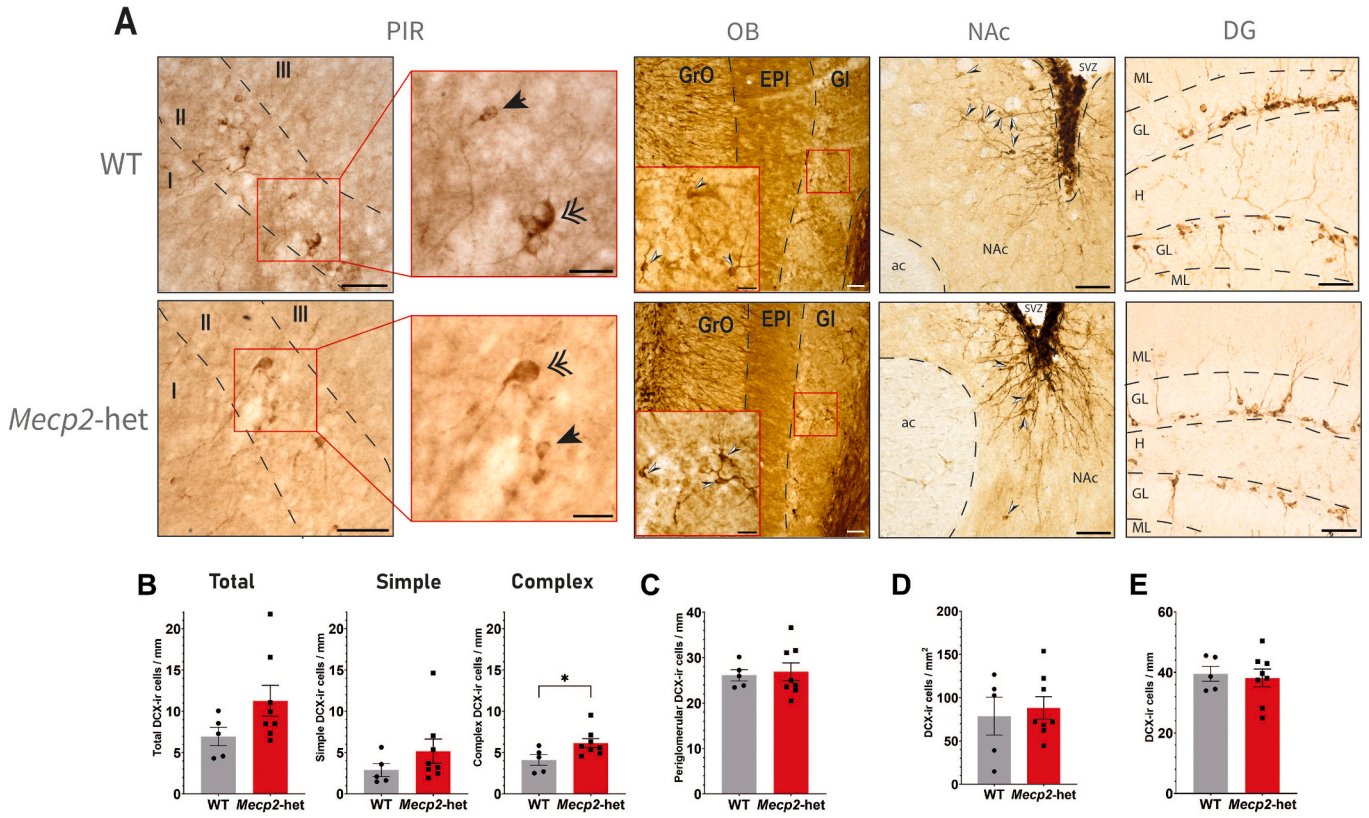

Fig. 1. Distribution and density of DCX-ir cells in WT and *Mecp2*-het female mice. (A) Representative images of DCX-ir neurons in the piriform cortex (simple arrows point to simple DCX-ir cells, double arrows point to complex cells), olfactory bulbs, nucleus accumbens and dentate gyrus of the hippocampus. Scale bar: 50 μm (inset: 20 μm). **(B, C, D, E)** Bar graphs comparing density of DCX-ir cells between WT (gray) and *Mecp2*-heterozygous (red) females in the piriform cortex **(B)**, periglomerular layer of the olfactory bulb **(C)**, nucleus accumbens **(D)** and dentate gyrus of the hippocampus. The comparison of DCX-ir cells in the Pir **(B)** has been performed considering all labelled cells (Total), and then separately considering the classification into simple (more immature), and complex (more mature), which are significantly increased in *Mecp2*-het females with respect to WT. Abbreviations: ac: anterior commissure; DG: dentate gyrus of the hippocampus; EPl: external plexiform layer of the olfactory bulb; Gl: periglomerular cell layer of the olfactory bulb; GrO: granular cell layer of the olfactory bulb; GL: granular layer of the dentate gyrus of the hippocampus; H: hilus; ML: molecular layer; SVZ: subventricular zone. All graphs represent mean ± Standard Error Mean (SEM), and individual values (dots). *: $p < 0.05$. (For interpretation of the references to colour in this figure legend, the reader is referred to the web version of this article.)

with a rudimentary one and a smaller soma size; and (2) "complex", larger cells with a larger and more developed dendritic tree (Rubio et al. 2016). Thus, in the Pir those DCX-ir cells with none or one neurite were classified as simple, whilst cells with two or more neurites were quantified as complex (Supplementary Fig. 1). In the DG, DCX-ir neurons were counted only in the granular layer, and their maximum somatic diameter was also measured manually. To evaluate neurons originated in the V-SVZ, we counted manually DCX-ir neurons in the periglomerular region of the OB (since the intense labelling in the granular cell layer precluded the quantification of individual cells), and in the NAc, where cells were counted in the region between the V-SVZ and the anterior commissure (aca). In addition, we measured the Euclidean distance from each DCX-ir cell located in the NAc to the nearest lateral ventricle wall as a measure of migratory capacity (García-González et al. 2021). Finally, DCX-ir cells were also inspected in the dorso-lateral region of the V-SVZ, at the CPu, where, as commented above, we could not distinguish individual DCX-ir cells (Supplementary Fig. 2). All quantifications were performed manually using Fiji software (NIH). Cell density was expressed as an average number of labelled cells per linear density or per area following Ghibaudi et al. (2023). The main diameter of each DCX-ir cell was measured manually with the straight-line tool in ImageJ as the greatest distance between two points in the surface of the cell that crosses through its centre (Esteve-Pérez et al. 2025).

Sholl and skeleton analyses

We examined the morphology of the DCX-ir cells from the Pir and the DG by means of Sholl and skeleton analysis using ImageJ SNT Plugin (default parameters, v4.2.1) and Analyze skeleton tool, respectively. First, cells from layer II of the Pir (complex only) and DG were drawn manually using a *camera lucida* attached to a Leica optic microscope. Neurons were selected only if they were relatively isolated from other neurons and without discernible breaks. Next, images were scanned and processed with ImageJ software to convert them to an 8-bit format and then skeletonized. We used Sholl method to quantify the number of intersections of the dendrites within concentric circles of increasing radius (radius steps set at 10 μm for Pir cells and 5 μm for DG cells, according to different neuronal arbour sizes) centred on the soma, and the total number of intersections. Complementary to Sholl, skeleton analysis was applied to examine several branching parameters, including total branch length, maximum branch length, number of junctions and number of branches. We analysed a total of 45 DCX-ir neurons of the Pir, and 70 DCX-ir neurons of the DG, with a minimum of 5 positive cells per animal.

Fractal analysis

To characterize structural complexity of DCX-ir neurons from the Pir (complex cells) and DG, we performed a fractal analysis. The binary images of outlined cells were then analysed using the ImageJ FracLac

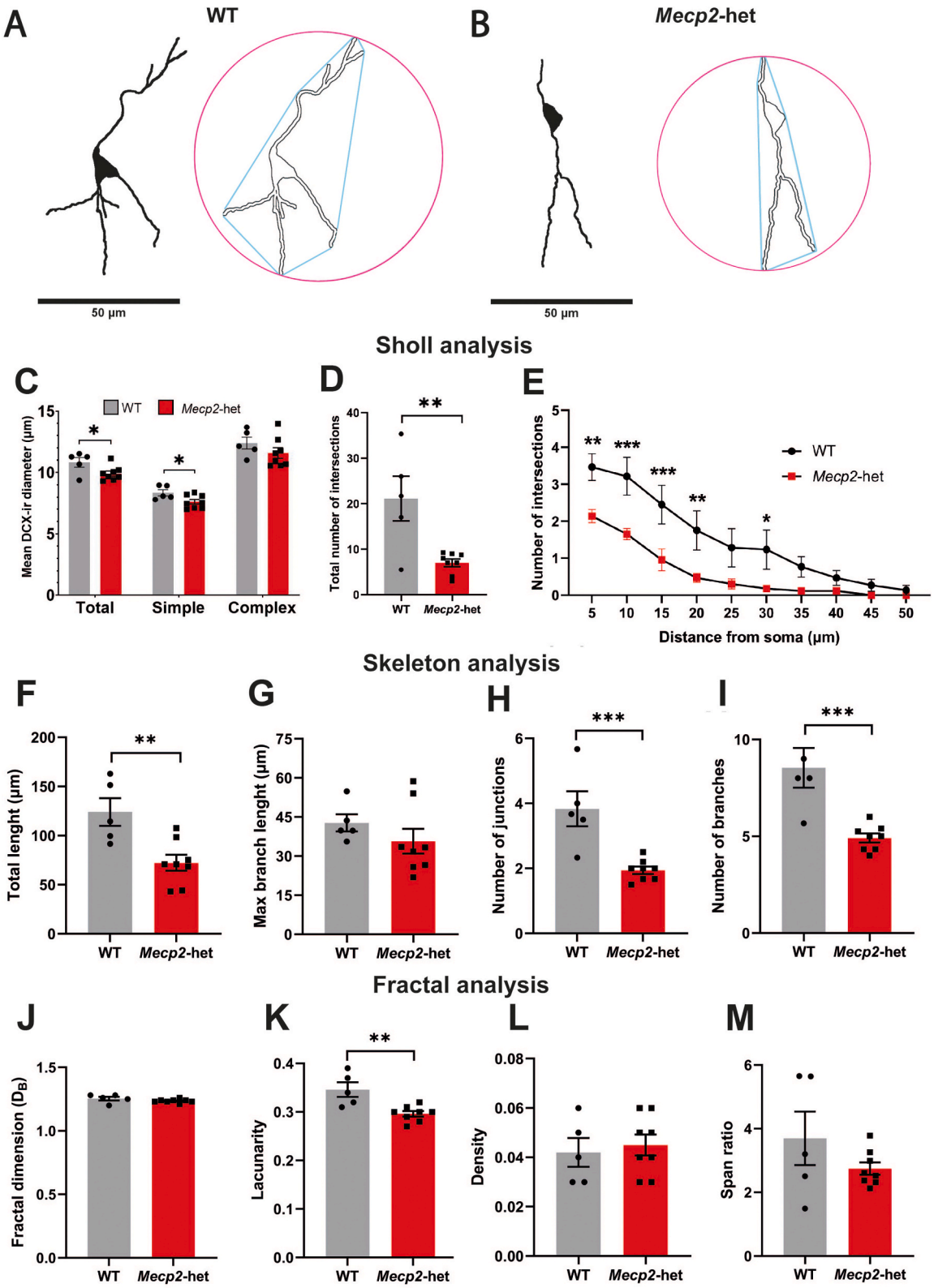

Fig. 2. Morphological analysis of DCX-ir cells in the Pir. A, B) Images depicting *camera lucida* drawings of DCX-ir cells of the Pir, along with their respective hull (blue) and circle (magenta) diagrams in WT **(A)** and *Mecp2*-het **(B)** mice. **C**) Main diameter of total, simple and complex DCX-ir neurons of the Pir revealed a significant decrease of this measure in *Mecp2*-het mice. **Sholl analysis** was performed measuring **(D)** the total number of intersections for DCX-ir neurons and **(E)** the number of intersections versus distance from the soma. **Skeleton analysis** was performed measuring **(F)** total dendritic length, **(G)** maximum branch length, **(H)** number of junctions and **(I)** number of branches. Finally, **fractal analysis** was assessed in terms of fractal dimension **(J)**, lacunarity **(K)**, density **(L)** and span ratio **(M)** calculations. These analyses reveal a shorter and less complex dendritic branching of DCX-ir cells of *Mecp2*-het females. All graphs represent mean ± Standard Error Mean (SEM). *: $p < 0.05$; **: $p < 0.01$; ***: $p < 0.005$. (For interpretation of the references to colour in this figure legend, the reader is referred to the web version of this article.)

plug-in. Changes in neuronal structure complexity were assessed by calculating Fractal dimension (D_B) and Lacunarity (λ). Fractal dimension provides a measure of complexity, which in turn is how a pattern's detail changes with the scale at which it is considered. Thus, it reflects how completely a neuronal arbour fills a specific area. Lacunarity is a measure of heterogeneity (rotational invariance) as a complement to complexity in describing digital images. Box-counting method was used for D_B and λ calculations. Default settings were left unchanged, except for Num G (the number of box counting grid orientations used during the scan), which was set at 5, following the recommended range indications from FracLac. Additional metrics included Hull and circle metrics data (Density and Span ratio).

Statistical analyses

Data were analysed using the GraphPad Prism 9 and R software. Data normality was tested with the Shapiro-Wilk test. To test statistical significance in multiple comparisons (number of intersections per radius in Sholl analysis), a two-way ANOVA followed by *post hoc* Bonferroni correction was employed. For two group comparisons, we used unpaired Student's *t-test* if normality was confirmed; otherwise, the Mann-Whitney test was used. All values are reported as mean ± SEM. Significance level was set at $p < 0.05$.

Results

Complex DCX-ir neurons are increased in the piriform cortex of Mecp2-heterozygous symptomatic females, but not in the neurogenic niches of DG or V-SVZ

As expected, we did not find qualitative differences in the distribution of DCX-ir cells between *Mecp2*-het and WT 6 months old female mice. Thus, DCX-ir cells were found in the Pir, OB, NAc and DG in both genotypes (Fig. 1A). Considering the finding of a restricted population of DCX-ir cells in the olfactory tubercle, which were increased in 2 months old *Mecp2*-null male mice (Martínez-Rodríguez et al. 2019), we also examined the olfactory tubercle in these samples. However, none or very few DCX-ir cells were found in this region in either genotype, suggesting that this population may be transient.

Quantitatively, we found no significant differences between genotypes in the total number of DCX-ir cells in the Pir ($t = -1.70$, $p = 0.11$; Fig. 1B). Remarkably, the linear density of DCX-ir cells in our samples of 6 months old mice closely resembles findings from an independent group analysing samples from mice of 5 to 7 months old (compare Fig. 1B in this study to Fig. 2C' in Ghibaudi et al. 2023), adding replicability to our study.

However, when considering the classification on simple (more immature) and complex (more mature), we found a significant increase in the density of complex DCX-ir cells in *Mecp2*-het females ($t = -2.32$, $p = 0.04$), but not in simple DCX-ir cells ($W = 11.0$, $p = 0.22$). In contrast, the density of DCX-ir cells did not differ between genotypes in the OB ($t = -0.28$, $p = 0.78$; Fig. 1C), or in the DG ($t = 0.33$, $p = 0.75$; Fig. 1E). Regarding DCX-ir cells that could migrate towards the striatum from the V-SVZ, we did not observe any difference between genotypes in the NAc ($t = -0.41$, $p = 0.69$; Fig. 1D). In addition, we did not find significant differences in the mean distance from DCX-ir cells to the V-SVZ ($W = 22.0$, $p = 0.83$; Data not shown). At the dorso-lateral region of the V-SVZ, we could not observe DCX-ir cells migrating towards the CPu (Supplementary Fig. 2). Altogether, these results suggest a region-specific effect of the heterozygosity of *Mecp2* in the Pir, without alterations in neurogenic areas.

Morphological analyses revealed decreased size and complexity in DCX-ir neurons of the piriform cortex

We next investigated whether *Mecp2* deficiency could affect the morphology and complexity of DCX-ir cells in the Pir. First, we measured the main somatic diameter of DCX-ir cells in the Pir, detecting a significant reduction in DCX-ir cells in *Mecp2*-het females compared to WT ($t = 2.24$, $p = 0.044$; Fig. 2C). This decrease might be largely due to a decrease in the main diameter of simple DCX-ir cells ($t = 2.37$, $p = 0.03$), while the main diameter of complex DCX-ir cells did not differ significantly between genotypes ($t = 1.2$, $p = 0.25$).

Further, Sholl analysis revealed a significant reduction in the total number of intersections in DCX-ir complex cells of *Mecp2*-het females when compared to their WT counterparts ($t = 3.58$; $p = 0.004$; Fig. 2D). As expected, the reduction was consistent across the entire dendritic profile, with statistically significant differences at 5, 10, 15, 20 and 30 μm from the cell somata (all $p < 0.05$) (Fig. 2E).

Skeleton analysis further confirmed a reduced dendritic complexity in *Mecp2*-het females, showing decreased total dendritic arbour length ($t = 3.45$, $p = 0.006$; Fig. 2F), fewer junctions ($t = 4.31$, $p = 0.001$, Fig. 2H), and fewer branches ($t = 4.29$, $p = 0.001$; Fig. 2I) as compared to WT.

Among the parameters measured by fractal and hull and circle analyses, only lacunarity, a measure of complexity of the dendritic tree, showed distinctive values between genotypes ($t = 3.64$, $p = 0.004$; Fig. 2K) which was driven by a significantly lower value in the *Mecp2*-het females. The rest of the measurement did not show differences between genotypes (all $p > 0.05$).

Morphological analyses revealed no significant effect of Mecp2 deficiency in DCX-ir neurons of the dentate gyrus

We performed the same morphological analyses in DCX cells in the DG of the hippocampus. In this case, none of the parameters evaluated by Sholl, skeleton or fractal analyses revealed significant differences between genotypes in DCX-ir cells of the DG (all $p > 0.05$, Fig. 3).

Discussion

In this study, we analysed the effect of *Mecp2* haploinsufficiency in distinct populations of immature neurons, namely the embryonic born DCX-ir cells of the Pir, and the continuously generated DCX-ir cells of the OB, the NAc and the DG. We found a specific increase in the density of DCX-ir cells in the Pir, as well as a reduced soma diameter, and less complex, shorter dendritic trees of these cells in *Mecp2*-het symptomatic females. In contrast, we did not find significant effects of *Mecp2* deficiency in DCX-ir cells of the OB, NAc or the DG. Together with our previous study showing specific deficits in the Pir in symptomatic *Mecp2*-null males but not pre-symptomatic *Mecp2*-het females (Martínez-Rodríguez et al. 2019), our data suggest that *Mecp2* deficiency contributes to arrested maturation of embryonic-born DCX-ir cells, which may be associated with the onset of overt symptoms.

These results are in agreement with previous studies revealing region-specific effects of *Mecp2* deficiency (Santos et al. 2010; Wang et al. 2013; Smith et al. 2019). Several factors may explain this regional specificity, including non-cell-autonomous effects of the function of MeCP2 (Kishi and Macklis 2004; Ballas et al. 2009), differential expression levels of MeCP2 in different regions (Cassel et al. 2004; Abellán-Álvaro et al. 2024) or regional differences in vulnerability to stress (Nacher et al. 2004; Abellán-Álvaro et al. 2024).

Probably the most important difference to consider between the populations studied here is the different ontogeny of these immature neurons. Thus, whereas new neurons are continuously being incorporated in the OB, NAc and DG of young adult mice (Doetsch et al. 1999; García-González et al. 2021; Arellano et al. 2024), immature neurons in the Pir are generated during embryonic development and remain immature until intrinsic and/or environmental factors trigger their maturation (Gómez-Climent et al. 2011; Rotheneichner et al. 2018; Abellán-Álvaro et al. 2024; Esteve-Pérez et al. 2025). These findings support the idea that MeCP2 is more likely to influence neuronal

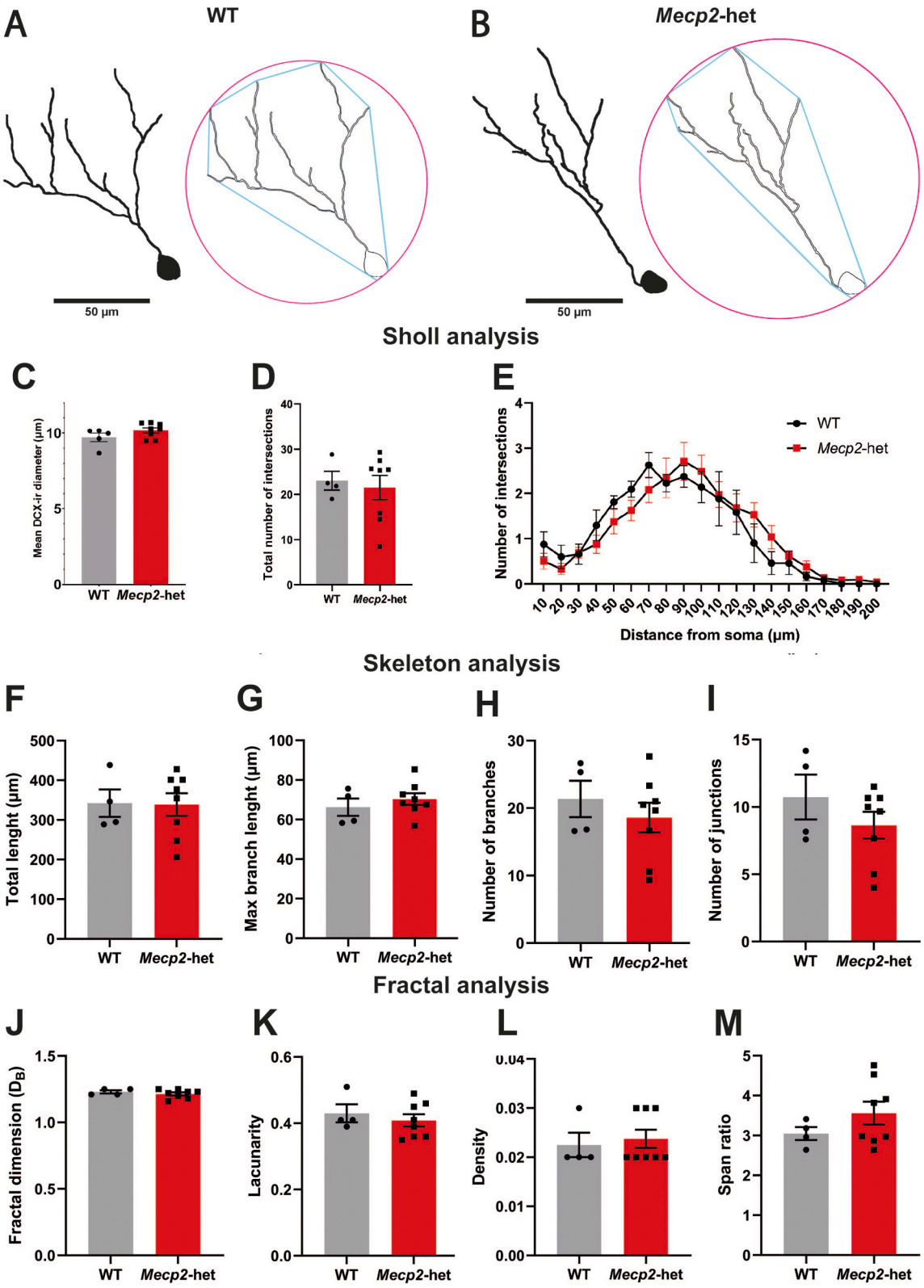

Fig. 3. Morphological analysis of DCX-ir cells in the hippocampal DG region. A, B) Images depicting camera lucida drawings of DCX-ir DG cells, along with their respective hull (blue) and circle (magenta) diagrams in **(A)** WT and **(B)** *Mecp2*-het mice. **C)** Main diameter of DCX-ir neurons of the DG. **Sholl analysis** was performed measuring **(D)** the total number of intersections for DCX-ir neurons and **(E)** the number of intersections versus distance from the soma. **Skeleton analysis** was performed measuring **(F)** total dendritic length, **(G)** maximum branch length, **(H)** number of junctions and **(I)** number of branches. Finally, **fractal analysis** was assessed in terms of fractal dimension **(J)**, lacunarity **(K)**, density **(L)** and span ratio **(M)** calculations. All graphs represent mean ± Standard Error Mean (SEM). (For interpretation of the references to colour in this figure legend, the reader is referred to the web version of this article.)

differentiation and maturation than for proliferation (Shahbazian 2002; Kishi and Macklis 2004; Smrt et al. 2007).

The olfactory system is a valuable system for studying neurodevelopment during healthy and pathological conditions, including RTT (Sweat and Cheetham 2024). Consequently, this system has been widely studied in both RTT patients and genetically modified mice. In RTT patients, nasal biopsies revealed fewer terminally differentiated olfactory receptor neurons and a notable increase in immature olfactory sensory neurons (Ronnett et al. 2003). In mouse models, previous studies in the olfactory system have found that delayed maturation caused by lack of *Mecp2* results in a transient abnormal axonal projections in the olfactory bulb and subglomerular disorganisation (Matarazzo et al. 2004). These results, together with those that show a postnatal deficit in the olfactory refinement in *Mecp2*-null males (Degano et al. 2014), suggest that an impairment in the RMS, which continuously brings newly generated neurons to the OB from the V-SVZ, might be occurring. However, we did not find significant effects of genotype in the density of DCX-ir cells in the periglomerular area *Mecp2*-het symptomatic mice, suggesting that postnatal neurogenesis in the V-SVZ towards this area is not affected by heterozygosity of *Mecp2*, despite the potential malfunctions in newly generated neurons in the OB (Matarazzo et al. 2004; Degano et al. 2014), or a subtle effect on transition to maturity such as the one we previously found in the *Mecp2*-null males (Martínez-Rodríguez et al. 2019).

On the other hand, immature neurons of the NAc, also arising from V-SVZ, have previously been related to chronic pain (García-González et al. 2021), and pain reception and behaviour is altered in both RTT patients and female rodent models (Downs et al. 2010; Cuitavi et al. 2025). The absence of differences in the density and migration distances of the V-SVZ in DCX-ir neurons in the NAc of *Mecp2*-het females suggests that other mechanisms and areas of pain processing could be involved in these deficits.

In addition to the increased density of complex DCX-ir cells in the Pir, we observed a reduction of dendritic arborization and complexity in the DCX-ir neurons of *Mecp2*-het females, in agreement with previous reports showing a dendritic and synaptic impairment in cortical neurons from both mouse models (Kishi and Macklis 2004; Belichenko et al. 2009) and RTT patients (Bauman et al. 1995; Belichenko et al. 1996). Moreover, some studies propose that soma size as a phenotypic marker of MeCP2 deficiency (Wang et al. 2013), and our data revealed that DCX-ir cells of the Pir of *Mecp2*-het females also had a smaller soma compared to WT females. Both the morphological impairment in these immature neurons of Pir and the increase of the density of complex DCX-ir cells in this region might compromise the reserve of cortical plasticity and glutamatergic input provided by these immature neurons. In this context, although the function of these immature neurons is still unclear (Rotheneichner et al. 2018), one could hypothesise that a delay in their maturation might impair the olfactory sensory and associative learning abilities of *Mecp2*-null mice. We previously demonstrated that *Mecp2*-null males are not anosmic, but display lower levels of olfactory investigation of neutral and social odours (Martínez-Rodríguez et al. 2020). Conversely, the putative olfactory deficits at peripheral level of these mice could delay the rate of maturation in brain olfactory regions (Martínez-Rodríguez et al., 2019). Future experiments are needed to demonstrate these hypotheses.

Finally, MeCP2 deficiency has been associated with structural and functional deficits in the hippocampus. For example, in RTT patients, impairment in the expression of *MECP2* has been associated with lower dendritic spine density in hippocampal mature cells (Chapleau et al. 2009; Nerli et al. 2020), whereas analogous studies in rodents have found how lack of *MECP2* induces morphological and synaptic alterations in mature neurons that leads to memory and learning deficits (Moretti and Zoghbi 2006), although without changes in the levels of proliferation in the DG (Smrt et al. 2007). As to newly generated neurons, a study showed that, in young adult male mice, *Mecp2*-KO new neurons of the DG that are already integrating in circuits within a niche of *MECP2*-expressing neurons exhibited less dendritic complexity and development (Sun et al. 2019). On the contrary, in our study, we failed to show morphological alterations in DCX-ir neurons in the DG of *Mecp2*-het females, likely because of the higher immaturity of these cells.

Limitations

Although our study reports quantitative and morphological differences in the DCX-ir population of the Pir between *Mecp2*-het and WT mice, we do not provide behavioural, electrophysiological or circuit-level data to back up functional interpretations. As such, ours is a descriptive study; however, together with our previous study in young *Mecp2*-mutant mice, our study supports the notion that MeCP2 is involved in the maturation process of neurons, and that deficits in this process are linked to the onset of an overt symptomatic phase in the mouse model of Rett.

In conclusion, our findings support the notion that the protracted maturation process of immature populations of embryonic origin is especially vulnerable to MeCP2 deficiency, whereas proliferative neurogenic sites might be less susceptible, at least in terms of density of DCX-ir cells. Future studies are needed to clarify the molecular causes of these local impairments and the potential consequences of these deficits in the neural networks. This way, we may contribute to identify new therapeutic targets aimed at promoting neuronal maturation in Rett syndrome.

CRediT authorship contribution statement

Rafael Esteve-Pérez: Writing – original draft, Methodology, Investigation. **Paloma Sevilla-Ferrer:** Writing – original draft, Methodology, Investigation. **Enrique Lanuza:** Writing – review & editing, Resources. **Vicente Herranz-Pérez:** Writing – review & editing, Conceptualization. **Jose V. Torres-Pérez:** Writing – review & editing, Writing – original draft, Supervision, Conceptualization. **Carmen Agustín-Pavón:** Writing – review & editing, Writing – original draft, Supervision, Project administration, Funding acquisition, Formal analysis, Data curation, Conceptualization.

Ethics approval

The study was approved by the Animal Experimentation Ethics Committee of the University of Valencia, Protocol 2019/VSC/PEA/0027, and carried out in strict accordance with EU directive 2010/63/EU.

Funding

Funded by Ayudas a la investigación en Síndrome de Rett, FinRett 2019 and 2022 to C.A-P. and Conselleria de Educación, Cultura, Universidades y Empleo from the Generalitat Valenciana (CIAICO/2023/027). JVTP is funded by the Spanish Ministry of Science, Innovation and Universities (MCIN/AEI/https://10.13039/501100011033) and the European Union "NextGenerationEU"/PRTR with a Ramón y Cajal contract (grant RYC2021-034012-I); JVTP is also supported by the Conselleria de Educación, Cultura, Universidades y Empleo from the Generalitat Valenciana with a Subvencion a grupos de investigación emergentes (grant CIGE/2024/73). Project carried out within the framework of the University of Valencia's Vice-Rectorate for Research internal programme, under the Special Actions call, file number UV-INV-AE-3651656. This work was also supported by the Conselleria de Educación, Cultura, Universidades y Empleo from the Generalitat Valenciana (CIPROM/2023/053) to VH-P. R.E-P is supported by a predoctoral fellowship from Conselleria de Educación, Cultura, Universidades y Empleo from the Generalitat Valenciana (ACIF2022/387).

Declaration of competing interest

The authors declare that they have no known competing financial interests or personal relationships that could have appeared to influence the work reported in this paper.

Acknowledgements

Authors are indebted to Dr Elena Martínez-Rodríguez and Josep Pardo-García for technical assistance, and to Dr María Martínez de Lagrán and Dr Emilio Varea for suggestions about Sholl analysis.

Appendix A. Supplementary data

Supplementary data to this article can be found online at https://doi.org/10.1016/j.neuroscience.2025.12.010.

References

Abellán-Álvaro, M., Stork, O., Agustín-Pavón, C., Santos, M., 2021. MeCP2 haplodeficiency and early-life stress interaction on anxiety-like behavior in adolescent female mice. J Neurodevelop Disord 13, 59. https://doi.org/10.1186/s11689-021-09409-7.

Abellán-Álvaro, M., Teruel-Sanchis, A., Madeira, M.F., et al., 2024. Doublecortin-immunoreactive neurons in the piriform cortex are sensitive to the long lasting effects of early life stress. Front. Neurosci. 18, 1446912. https://doi.org/10.3389/fnins.2024.1446912.

Amir, R.E., Van Den Veyver, I.B., Wan, M., et al., 1999. Rett syndrome is caused by mutations in X-linked MECP2, encoding methyl-CpG-binding protein 2. Nat. Genet. 23, 185–188. https://doi.org/10.1038/13810.

Arellano, J.I., Duque, A., Rakic, P., 2024. A coming-of-age story: adult neurogenesis or adolescent neurogenesis in rodents? Front. Neurosci. 18, 1383728. https://doi.org/10.3389/fnins.2024.1383728.

Ballas, N., Lioy, D.T., Grunseich, C., Mandel, G., 2009. Non–cell autonomous influence of MeCP2-deficient glia on neuronal dendritic morphology. Nat. Neurosci. 12, 311–317. https://doi.org/10.1038/nn.2275.

Bauman, M., Kemper, Th., Arin, D., 1995. Microscopic Observations of the Brain in Rett Syndrome. Neuropediatrics 26, 105–108. https://doi.org/10.1055/s-2007-979737.

Belichenko, P.V., Fedorov, A.A., Dahlström, A.B., 1996. Quantitative analysis of immunofluorescence and lipofuscin distribution in human cortical areas by dual-channel confocal laser scanning microscopy. J. Neurosci. Methods 69, 155–161. https://doi.org/10.1016/S0165-0270(96)00035-0.

Belichenko, P.V., Wright, E.E., Belichenko, N.P., et al., 2009. Widespread changes in dendritic and axonal morphology in *Mecp2* -mutant mouse models of rett syndrome: evidence for disruption of neuronal networks. J of Comparative Neurology 514, 240–258. https://doi.org/10.1002/cne.22009.

Benedetti, B., Dannehl, D., König, R., et al., 2020. Functional Integration of Neuronal Precursors in the Adult Murine Piriform Cortex. Cereb. Cortex 30, 1499–1515. https://doi.org/10.1093/cercor/bhz181.

Canton, A.P.M., Tinano, F.R., Guasti, L., et al., 2023. Rare variants in the MECP2 gene in girls with central precocious puberty: a translational cohort study. The Lancet Diabetes & Endocrinology 11, 545–554. https://doi.org/10.1016/S2213-8587(23)00131-6.

Cassel, S., Revel, M.-O., Kelche, C., Zwiller, J., 2004. Expression of the methyl-CpG-binding protein MeCP2 in rat brain. An Ontogenetic Study. Neurobiology of Disease 15, 206–211. https://doi.org/10.1016/j.nbd.2003.10.011.

Chapleau, C.A., Calfa, G.D., Lane, M.C., et al., 2009. Dendritic spine pathologies in hippocampal pyramidal neurons from Rett syndrome brain and after expression of Rett-associated MECP2 mutations. Neurobiol. Dis. 35, 219–233. https://doi.org/10.1016/j.nbd.2009.05.001.

Coviello, S., Gramuntell, Y., Klimczak, P., et al., 2022. Phenotype and distribution of Immature Neurons in the Human Cerebral Cortex Layer II. Front. Neuroanat. 16, 851432. https://doi.org/10.3389/fnana.2022.851432.

Cuitavi, J., Martínez-Rodríguez, E., Abellán-Álvaro, M., et al., 2025. Longitudinal Analysis in Mecp2-het Female mice reveals Atypical Nociceptive Behaviours. In press, J Mol Med.

Degano, A.L., Park, M.J., Penati, J., et al., 2014. MeCP2 is required for activity-dependent refinement of olfactory circuits. Mol. Cell. Neurosci. 59, 63–75. https://doi.org/10.1016/j.mcn.2014.01.005.

Doetsch, F., Caillé, I., Lim, D.A., et al., 1999. Subventricular Zone Astrocytes are Neural Stem Cells in the Adult Mammalian Brain. Cell 97, 703–716. https://doi.org/10.1016/S0092-8674(00)80783-7.

Downs, J., Géranton, S.M., Bebbington, A., et al., 2010. Linking *MECP2* and pain sensitivity: the example of Rett syndrome. American J of Med Genetics Pt A 152A, 1197–1205. https://doi.org/10.1002/ajmg.a.33314.

Esteve-Pérez, R., Abellán-Álvaro, M., Navarro-Moreno, C., et al., 2025. The density of doublecortin cells in the piriform cortex is affected by transition to adulthood but not first pregnancy in mice. Brain Struct. Funct. 230, 94. https://doi.org/10.1007/s00429-025-02957-x.

García-González, D., Dumitru, I., Zuccotti, A., et al., 2021. Neurogenesis of medium spiny neurons in the nucleus accumbens continues into adulthood and is enhanced by pathological pain. Mol. Psychiatry 26, 4616–4632. https://doi.org/10.1038/s41380-020-0823-4.

Ghibaudi, M., Marchetti, N., Vergnano, E., et al., 2023. Age-related changes in layer II immature neurons of the murine piriform cortex. Front. Cell. Neurosci. 17, 1205173. https://doi.org/10.3389/fncel.2023.1205173.

Gómez-Climent, M.Á., Hernández-González, S., Shionoya, K., et al., 2011. Olfactory bulbectomy, but not odor conditioned aversion, induces the differentiation of immature neurons in the adult rat piriform cortex. Neuroscience 181, 18–27. https://doi.org/10.1016/j.neuroscience.2011.03.004.

Guy, J., Hendrich, B., Holmes, M., et al., 2001. A mouse Mecp2-null mutation causes neurological symptoms that mimic Rett syndrome. Nat. Genet. 27, 322–326. https://doi.org/10.1038/85899.

Kishi, N., Macklis, J.D., 2004. MECP2 is progressively expressed in post-migratory neurons and is involved in neuronal maturation rather than cell fate decisions. Mol. Cell. Neurosci. 27, 306–321. https://doi.org/10.1016/j.mcn.2004.07.006.

La Rosa C, Cavallo F, Pecora A, et al (2020) Phylogenetic variation in cortical layer II immature neuron reservoir of mammals. eLife 9:e55456. 10.7554/eLife.55456.

Li YN, Hu DD, Cai XL, et al (2023) Doublecortin-Expressing Neurons in Human Cerebral Cortex Layer II and Amygdala from Infancy to 100 Years Old. Mol Neurobiol. 2023 Jun;60(6):3464-3485. http://doi: 10.1007/s12035-023-03261-7.

Martínez-Rodríguez, E., Martín-Sánchez, A., Coviello, S., et al., 2019. Lack of MeCP2 leads to region-specific increase of doublecortin in the olfactory system. Brain Struct. Funct. 224, 1647–1658. https://doi.org/10.1007/s00429-019-01860-6.

Martínez-Rodríguez, E., Martín-Sánchez, A., Kul, E., et al., 2020. Male-specific features are reduced in Mecp2-null mice: analyses of vasopressinergic innervation, pheromone production and social behaviour. Brain Struct. Funct. 225 (7), 2219–2238. https://doi.org/10.1007/s00429-020-02122-6.

Matarazzo, V., Cohen, D., Palmer, A.M., et al., 2004. The transcriptional repressor Mecp2 regulates terminal neuronal differentiation. Mol. Cell. Neurosci. 27, 44–58. https://doi.org/10.1016/j.mcn.2004.05.005.

Moretti, P., Zoghbi, H.Y., 2006. MeCP2 dysfunction in Rett syndrome and related disorders. Curr. Opin. Genet. Dev. 16, 276–281. https://doi.org/10.1016/j.gde.2006.04.009.

Nacher, J., Crespo, C., McEwen, B.S., 2001. Doublecortin expression in the adult rat telencephalon. Eur J of Neuroscience 14, 629–644. https://doi.org/10.1046/j.0953-816x.2001.01683.x.

Nacher, J., Pham, K., Gil-Fernandez, V., McEwen, B.S., 2004. Chronic restraint stress and chronic corticosterone treatment modulate differentially the expression of molecules related to structural plasticity in the adult rat piriform cortex. Neuroscience 126, 503–509. https://doi.org/10.1016/j.neuroscience.2004.03.038.

Nan, X., Campoy, F.J., Bird, A., 1997. MeCP2 is a Transcriptional Repressor with Abundant Binding Sites in Genomic Chromatin. Cell 88, 471–481. https://doi.org/10.1016/S0092-8674(00)81887-5.

Nerli, E., Roggero, O.M., Baj, G., Tongiorgi, E., 2020. In vitro modeling of dendritic atrophy in Rett syndrome: determinants for phenotypic drug screening in neurodevelopmental disorders. Sci. Rep. 10, 2491. https://doi.org/10.1038/s41598-020-59268-w.

Paredes, M.F., Sorrells, S.F., Garcia-Verdugo, J.M., Alvarez-Buylla, A., 2016. Brain size and limits to adult neurogenesis. J of Comparative Neurology 524, 646–664. https://doi.org/10.1002/cne.23896.

Paxinos, G., Franklin, K.B.J., 2012. Paxinos and Franklin's the mouse brain in stereotaxic coordinates, Fourth edition. Academic Press.

Paxinos, G., Franklin, K.B.J., 2019. Paxinos and Franklin's the mouse brain in stereotaxic coordinates, Fifth edition. Academic Press, an imprint of Elsevier, London.

Ronnett, G.V., Leopold, D., Cai, X., et al., 2003. Olfactory biopsies demonstrate a defect in neuronal development in Rett's syndrome. Ann. Neurol. 54, 206–218. https://doi.org/10.1002/ana.10633.

Rotheneichner, P., Belles, M., Benedetti, B., et al., 2018. Cellular Plasticity in the Adult Murine Piriform Cortex: Continuous Maturation of Dormant Precursors into Excitatory Neurons. Cereb. Cortex 28, 2610–2621. https://doi.org/10.1093/cercor/bhy087.

Rubio, A., Belles, M., Belenguer, G., et al., 2016. Characterization and isolation of immature neurons of the adult mouse piriform cortex. Dev. Neurobiol. 76, 748–763. https://doi.org/10.1002/dneu.22357.

Santos, M., Summavielle, T., Teixeira-Castro, A., et al., 2010. Monoamine deficits in the brain of methyl-CpG binding protein 2 null mice suggest the involvement of the cerebral cortex in early stages of Rett syndrome. Neuroscience 170, 453–467. https://doi.org/10.1016/j.neuroscience.2010.07.010.

Santos, M., Temudo, T., Kay, T., et al., 2009. Mutations in the *MECP2* Gene are not a Major Cause of Rett Syndrome-like or Related Neurodevelopmental Phenotype in Male patients. J. Child Neurol. 24, 49–55. https://doi.org/10.1177/0883073808321043.

Shahbazian, M.D., 2002. Insight into Rett syndrome: MeCP2 levels display tissue- and cell-specific differences and correlate with neuronal maturation. Hum. Mol. Genet. 11, 115–124. https://doi.org/10.1093/hmg/11.2.115.

Sharifi, O., Yasui, D.H., 2021. The Molecular Functions of MeCP2 in Rett Syndrome Pathology. Front. Genet. 12, 624290. https://doi.org/10.3389/fgene.2021.624290.

Smith, E.S., Smith, D.R., Eyring, C., et al., 2019. Altered trajectories of neurodevelopment and behavior in mouse models of Rett syndrome. Neurobiol. Learn. Mem. 165, 106962. https://doi.org/10.1016/j.nlm.2018.11.007.

Smrt, R.D., Eaves-Egenes, J., Barkho, B.Z., et al., 2007. Mecp2 deficiency leads to delayed maturation and altered gene expression in hippocampal neurons. Neurobiol. Dis. 27, 77–89. https://doi.org/10.1016/j.nbd.2007.04.005.

Sorrells, S.F., Paredes, M.F., Cebrian-Silla, A., et al., 2018. Human hippocampal neurogenesis drops sharply in children to undetectable levels in adults. Nature 555, 377–381. https://doi.org/10.1038/nature25975.

Sun, Y., Gao, Y., Tidei, J.J., et al., 2019. Loss of MeCP2 in immature neurons leads to impaired network integration. Hum. Mol. Genet. 28, 245–257. https://doi.org/10.1093/hmg/ddy338.

Sweat, S.C., Cheetham, C.E.J., 2024. Deficits in olfactory system neurogenesis in neurodevelopmental disorders. Genesis 62, e23590. https://doi.org/10.1002/dvg.23590.

Torres-Pérez, J.V., Martínez-Rodríguez, E., Forte, A., et al., 2022. Early life stress exacerbates behavioural and neuronal alterations in adolescent male mice lacking methyl-CpG binding protein 2 (Mecp2). Front. Behav. Neurosci. 16, 974692. https://doi.org/10.3389/fnbeh.2022.974692.

Wang, I.-T.-J., Reyes, A.-R.-S., Zhou, Z., 2013. Neuronal morphology in MeCP2 mouse models is intrinsically variable and depends on age, cell type, and Mecp2 mutation. Neurobiol. Dis. 58, 3–12. https://doi.org/10.1016/j.nbd.2013.04.020.

Whitman, M.C., Greer, C.A., 2009. Adult neurogenesis and the olfactory system. Prog. Neurobiol. 89, 162–175. https://doi.org/10.1016/j.pneurobio.2009.07.003.